Hindawi
Advances in Mathematical Physics
Volume 2022, Article ID 6271265, 11 pages
https://doi.org/10.1155/2022/6271265

Research Article

Approximate Analytical Study of Time-Dependent MHD Casson Hybrid Nanofluid over a Stretching Sheet and Considering Thermal Radiation

Ali Rehman,[1] Zabidin Salleh,[1] Abd Allah A. Mousa,[2] Ebenezer Bonyah,[3] and Waris Khan[4]

[1]*Department of Mathematics, Faculty of Ocean Engineering Technology and Informatics, Universiti Malaysia Terengganu, 21030 Kuala Nerus, Terengganu, Malaysia*
[2]*Department of Mathematics and Statistics, College of Science, Taif University, P.O. Box 11099, Taif 21944, Saudi Arabia*
[3]*Department of Mathematics Education, Akenten Appiah Menka University of Skills Training and Entrepreneurial Development (Kumasi Campus), Ghana*
[4]*Department of Mathematics and Statistics, Hazara University, Mansehra, 21120 Khyber Pakhtunkhwa, Pakistan*

Correspondence should be addressed to Ebenezer Bonyah; ebbonya@gmail.com

Received 6 October 2021; Revised 13 February 2022; Accepted 12 April 2022; Published 13 May 2022

Academic Editor: Zine El Abiddine Fellah

The heat transfer ratio plays an important role in the production sector, and hybrid nanofluid has more heat transfer as compared to the base fluid. Two sorts of hybrid nanofluids have been used for heat enhancement applications. The present research paper is aimed at investigating an approximate analytical study of time-dependent MHD Casson hybrid nanofluid on an extending surface along with thermal radiation. The novelty of present research is that the first time-dependent Casson MHD flow of hybrid is addressed analytically in the form of a series solution along with flexible properties on an extending surface. Transforming the nonlinear partial differential equation to nonlinear ordinary differential equation, we used the defined similarity transformation. The governing nonlinear equations are solved with help of the approximate analytical method presented by Liao. The impact of different parameters like Casson parameter, unsteady parameter, magnetic field parameter, porosity parameter, Prandtl number, Eckert number, radiation parameter, and Grashof number is presumed in the form figures for velocity and temperature profile. The current research article has a good comparison with the previously published work.

1. Introduction

In engineering processes, magneto hydrodynamics (MHD) has important applications, for example, design of a cooling system, liquid system, cooling of the nuclear reactor, thermal insulators, geothermal system, polymer, petroleum, and blood-pumping machines. The researcher takes more interest in the problem involved in chemical reaction on unsteady MHD-free convection flow, due to some important application in numerous industrial methods. Mekheimer [1] studies convection flow with the induced magnetic field by using peristaltic flow. Ellahi and Riaz [2] investigate MHD flow with the help of third grad fluid. Mukhopadhyay and Gorla [3] study time-dependent magneto hydrodnamics boundary layer flow by using moveable surface. The study of non-Newtonian fluids has more important as compared to Newtonian fluid, due to the inclusive variety application in organic field such blood at little sheer rate suspension, muds, chime, apple sauce, honey, and shampoos. These are the many applications of non-Newtonian fluids, the mathematical problem for Casson fluid is presented to investigate the mechanism of pseudoplastic yield stress liquids. Nadeem et al. [4] used linearly extending sheet to discuss 3D Casson fluid. Benazir et al. [5] used vertical cone and flat with

nonuniform heat source to study unsteady magneto hydynamics Casson fluid flow in this study, and they show that growth of the Casson fluid parameter decreases liquid flow and increases shear stress in the flow system. Nowadays, for energy resources, nanofluids are the effective agents. These fluids are used for improvement temperature spread devices used in several industries and engineering fields. It is not sufficient to acquire energy but to control absorptions of energy so can only solve this problem one to agree advance heat transfer fluids to rheostat the expenses of energy and the development the maximum heat transfer which is the requirement of the manufacturing and other related scientific arenas. The study of nanofluid is more important due to some key application in different parts of industries because of high heat transfer ratio. Parmar et al. [6] investigate the Casson flow and blood flow. Nadeem et al. [7] investigate the consequence of radioactivity for Casson fluid. Ullah et al. [8] used porous sheet to study the non-Newtonian fluid flow. Kamran et al. [9] investigate Casson nanofluid flow numerical along with joule heating and slip effect. Archana et al. [10] study the consequence of radiation on the energy expression of Casson fluid. Gireesha et al. [11] study the impression of Casson nanofluid flow and chemical reaction. Numerous other investigations are related to the Casson fluid, Souayeh et al. [12], Ullah et al. [13], and Aziz and Afify [14]. In the view of the above study, recently, several revisions have been conducted around the nanofluid, but the researchers take more interest in the new type introduced nanofluid known as hybrid nanofluid. Hybrid nanofluid is defined as two or more types of nanofluid are suspended in the base fluid. The interest of the researchers in this subject is the high heat transfer ratio improvement and invention rate saving that can be attained by the using these nanofluids. The researchers take more interest in this new type of nanofluids to solve the problems of real world. Initially, the idea of hybrid nanofluid increases the advanced structures of usual nanofluid was investigated by Suresh et al. [15]. Devi and Devi [16, 17] used to move surface to investigate the problems of MHD hybrid nanofluid. Tayebi and Chamkha [18] used an annulus to study the heat transfer of hybrid nanofluid. Ghadikolaei et al. [19] study the features of TiO_2-Cu/H_2O a hybrid nanofluid in the presence of resistance force. Hayat et al. [20] used the rotating disc to study flow Ag-CuO/water hybrid nanofluid. Yousefi et al. [21] used stretching cylinder to study the stagnation point flow of aqueous titanic-copper hybrid. Subhani and Nadeem [22] used stretching surface to study the behavior of Cu-TiO_2/H_2O hybrid nanofluid. Li et al. [23] under seismic conditions examine modeling response of magnetorheological fluid dampers. The influence of MHD (magneto hydrodynamics) flow of Casson fluid is examined by Crane et al. [24]. Nadeem et al. [25] used stretching sheet to examine the 2D viscous fluid flow. The mass diffusion on MHD (magneto hydrodynamics) flow over a moveable surface was deliberated by Ali and Sandeep [26]. The unsteady Casson fluid over extending sheet was studied by Vyas and Ranjan [27]. Chamka and Takhar [28] studied the MHD flow on nonlinear extending surface by permeable surface. Sandhya et al. [29] discuss buoyancy forces and activation energy on the MHD radiative flow over an exponentially stretching sheet. Lund et al. [30] study double comparison of MHD flow of Casson fluid. Ibrahim and Anbessa [31] study 3D MHD flow of nanofluid along with ion slip effects. Varun Kumar et al. [32] used stretching surface to investigate modeling on Casson nanofluid flow along with the influence of magnetic field. Yusuf et al. [33] study magneto-bioconvection flow of Williamson nanofluid over an inclined plate with gyro tactic microorganisms and entropy generation. Kumar et al. [34] study the impact of thermophoretic element testimony heat transmission through the dynamics of Casson fluid flow on a stretching needle. Rehman and Salleh [35] used stretching surface to study effect on MHD flow and heat transmission on hybrid nanofluids. Rehman and Salleh [36] used stretching surface to study time-dependent boundary layer stagnation point flow of nanofluid. The purpose of the present research paper is to investigate approximate analytical study of time-dependent MHD Casson hybrid nanofluid on an extending surface along with thermal radiation. The novelty of present research paper is that the first time-dependent Casson MHD flow of hybrid is addressed along with variable properties over stretching surface and the approximate solution one for velocity and other for temperature profile is analyzed by analytical method. Two sorts of hybrid nanofluids TiO_2 + Ag + blood and TiO_2+blood are heat enhancement applications. Transforming the nonlinear partial differential equation to nonlinear ordinary differential equation, we used the defined similarity transformation. The governing nonlinear ODE (ordinary differential equations) is solving with approximate analytical method [37]. With the help of graphs, the influence of dissimilar parameters is presented. Also the consequence of C_f and Nu are obtainable in the form of tables. The current research article has good comparison with the already published work.

2. Mathematical Formulation

The two-dimensional time-dependent incomparable laminar boundary layer MHD flow of hybrid nanofluid over a permeable inclined movable surface. The impact in density difference with temperature only arises on the body force term, and later, changed temperature induces the buoyancy forces. The velocity of the moving surface in the direction of applied force in x direction is $u_w(x,t)$, and the mass transfer is $v_w(t)$ which is normal to the moving surface. The surface (wall) temperature is $T_w(x,t)$, and uniform temperature away from the moving surface is T_∞. Under these assumptions, the governing model equations are as follows:

$$\frac{\partial u}{\partial x} + \frac{\partial v}{\partial y} = 0, \tag{1}$$

$$\frac{\partial u}{\partial t} + u\frac{\partial u}{\partial x} + v\frac{\partial u}{\partial y} = \left(1 + \frac{1}{\beta}\right)\frac{\partial^2 u}{\partial y^2} - \frac{\sigma_{hnf}}{\rho_{hnf}}B_0^2(t)u + g(T - T_\infty)\cos\alpha, \tag{2}$$

$$\frac{\partial T}{\partial t}+u\frac{\partial T}{\partial x}+u\frac{\partial T}{\partial y}=\frac{k_{hnf}}{\left(\rho C_p\right)_{hnf}}\frac{\partial^2 T}{\partial y^2}-\frac{1}{\left(\rho C_p\right)_{hnf}}\frac{\partial q_r}{\partial y}+\left(\frac{\mu_{hnf}}{\rho C_p}\right)_{hnf}\left(\frac{\partial u}{\partial y}\right)^2+\frac{\sigma_{hnf}}{\left(\rho C_p\right)_{hnf}}B_0^2(t)u^2, \tag{3}$$

where t represents time, u and v represent velocity in x and y directions, ρ_{hnf} is the density of the hybrid nanofluid, μ_{hnf} represents the coefficient of viscosity, C_p represents the specific heat, β_T is the convection term, T is the temperature of the wall, and T_∞ is temperature away from the surface; the kinematic viscosity of the hybrid nanofluid is denoted by ν_{hnf}, the electrical conductivity of the hybrid nanofluid is σ_{hnf}, the strength of the external magnetic field is denoted by B_0, and q_r is the radiation heat flux. The relevant boundary condition is given below.

$$\begin{aligned} u=u_w(x,t)&=\frac{cx}{1-\lambda t},\\ v&=v_w(t),\\ T&=T_w(x,t),\\ y&=0,\\ u&\longrightarrow o,\\ T&\longrightarrow T_\infty,\\ y&\longrightarrow \infty. \end{aligned} \tag{4}$$

In Equation (4), c represents the early extending rate, λ represents constant, and the subscripts w and ∞ are attitude for surface and boundary layer edge. To convert the nonlinear partial differential equation (Equations (1) and (2)) to nonlinear ordinary differential equation, we used the following similarity transformation.

$$\begin{aligned} \eta&=\sqrt{\frac{c}{\nu^*(1-\lambda t)}}y,\\ \psi&=\sqrt{\frac{\nu^* c}{(1-\lambda t)}}xf(\eta),\\ \theta(\eta)&=\frac{T-T_\infty}{T_w-T_\infty}. \end{aligned} \tag{5}$$

Using Equation (5) in Equations (1)–(3), Equation (5) satisfied Equation (1) identically, and convert Equations (2) and (3) to the following form.

$$\frac{(1-\phi_1-\phi_2)^{-2.5}}{(1-\phi_1-\phi_2)+\phi_1\left(\rho_1/\rho_f\right)+\phi_2\left(\rho_2/\rho_f\right)}\left(1+\frac{1}{\beta}\right)f'''-S\left(f'+\frac{\eta}{2}f''\right)-(1-\phi_1)^{2.5}(1-\phi_1)^{2.5}[\varphi+M]f'-\left(f'\right)^2+ff''+G_r\theta=0, \tag{6}$$

$$\frac{(1-\phi_1-\phi_2)^{-2.5}}{(1-\phi_1-\phi_2)+\phi_1\left(\rho_1/\rho_f\right)+\phi_2\left(\rho_2/\rho_f\right)}\frac{k_s}{k_{hnf}}\theta''+\frac{\beta_1\left(\theta'\right)^2+(1-\phi_1)^{2.5}(1-\phi_1)^{2.5}\Pr\left[S(\eta/2)\theta'+2S\theta+f'\theta-f\theta'-\mathrm{Ec}\left(f''\right)^2\right]}{(1+R+\beta_1\theta)}. \tag{7}$$

The transform boundary conditions for the defined problem are as follows:

$$\begin{aligned} f(0)&=0,\\ f'(0)&=1,\\ \theta(0)&=1,\\ f'(\infty)&=0,\\ \theta'(\infty)&=0, \end{aligned} \tag{8}$$

where S, φ, M, G_r, Pr, R, Ec, and β are time-dependent parameter, porous medium parameter, magnetic parameter, Grashof number, Prandtl number, radiation parameter, Eckert number, and Casson parameter and defined in

$$\begin{aligned} S&=\frac{\lambda}{c},\\ \varphi&=\frac{\nu^*(1-\lambda t)}{k^* c},\\ M&=\frac{\sigma B_0^2(1-\lambda t)}{\rho c},\\ G_r&=\frac{g\beta_T x(T_w-T_\infty)}{u_w^2}\cos\alpha,\\ \Pr&=\frac{\nu}{\alpha},\\ \mathrm{Ec}&=\frac{u_w^2}{C_p(T_w-T_\infty)}. \end{aligned} \tag{9}$$

The skin friction in x and y directions is as follows:

$$\mathrm{Re}_x^{1/2}C_{hnf}=-\frac{(1-\phi_1-\phi_2)^{-2.5}}{(1-\phi_1-\phi_2)+\phi_1\left(\rho_1/\rho_f\right)+\phi_2\left(\rho_2/\rho_f\right)}f''(0). \tag{10}$$

Nusselt number and Sherwood number is given by

$$\mathrm{Re}_x^{-1/2}\mathrm{Nu}_x=-\frac{k_s}{k_{hnf}}\theta'(0), \tag{11}$$

2.1. OHAM Solution. The model governing Equations (6) and (7) is analyzed with the help of approximate analytical OHAM

$$E(w(\eta))+J(w(\eta))+r(\eta)=0,\ C(w(\eta)=0). \tag{12}$$

Table 1: The inspiration of M and β on skin friction coefficient.

β	M	TiO_2+Ag+blood	TiO_2+blood
0.1	1	0.5223	0.3137
0.2	2	0.5573	0.3418
0.3	3	0.5911	0.3756
0.4	4	0.6317	0.4434
0.5	5	0.6794	0.4754
0.6	6	0.7521	0.5316
0.7	7	0.7965	0.5641

Table 2: Inspiration of R and Ec on Nusselt number.

R	Ec	TiO_2+Ag+blood	TiO_2 + blood
0.5	1	0.2123	0.6071
1	2	0.2934	0.6825
1.5	3	0.3745	0.7037
2	4	0.3956	0.7563
2.5	5	0.4376	0.7912
3	6	0.4959	0.8025
3.5	7	0.5502	0.8341

Table 3: Convergence control parameter for particular method.

m	ε_m^f TiO_2 + Ag + blood	ε_m^θ TiO_2 + Ag + blood
5	0.6438×10^{-1}	0.6775×10^{-3}
10	0.4094×10^{-2}	0.1873×10^{-5}
15	0.9443×10^{-3}	0.9729×10^{-7}
20	0.7298×10^{-5}	0.5413×10^{-8}
25	0.5787×10^{-7}	0.1442×10^{-9}

Table 4: Convergence control parameter for particular method.

m	ε_m^f TiO_2 + blood	ε_m^θ TiO_2 + blood
5	0.7991×10^{-1}	0.8574×10^{-1}
10	0.5266×10^{-3}	0.5759×10^{-2}
15	0.1138×10^{-5}	0.8759×10^{-5}
20	0.9616×10^{-6}	0.3721×10^{-7}
25	0.5133×10^{-9}	0.6632×10^{-9}

In Equation (12), E represents linear operator, η represents the independent variable, $r(\eta)$ represents the unknown function, J represents the nonlinear operator, and $C(\omega)$ represents the boundary operator for the problem.

The initial solution for the defined $f'(\eta)$ and $\theta(\eta)$ is

$$f_0(\eta) = \eta^3 + e^{-\eta}, \tag{13}$$

Table 5: Comparison for $f'(\eta)$. And publish work.

m	Numerical	Analytical	Error
1	1	1	0
2	1.52….	1.50….	0.02…
3	1.31….	1.29….	0.02…
4	1.46….	1.44….	0.02…
5	0.57….	0.53….	0.04…
6	0.73….	0.71….	0.02…
7	0.79….	0.77….	0.02…
8	0.89….	0.88….	0.01…
9	0.32….	0.27….	0.05…
10	0.52….	0.50….	0.02…

$$\theta_0(\eta) = \frac{1}{2} e^{-\eta}. \tag{14}$$

These two initial guess are obtained with the help of linear operator.

$$E_f = f''' + ff'' = 0, E_\theta = \theta'' = 0. \tag{15}$$

The residual error for Equations (6) and (7) is defined by Liao [37].

$$\varepsilon_m^f = \frac{1}{n_1 + 1} \sum_{j_1=1}^{n_1} \left[\kappa_f \left(\sum_{j_1=1}^{n_1} f_1(\eta)_{\eta = j\delta\eta} \right) \right], \tag{16}$$

$$\varepsilon_m^\theta = \frac{1}{n+1} \sum_{j=1}^{n} \left[\kappa_\theta \left(\sum_{j=1}^{n} f(\eta)_{\eta = j\delta\eta}, \sum_{j=1}^{n} \theta(\eta)_{\eta = j\delta\eta} \right) \right], \tag{17}$$

$$\varepsilon_m^t = \varepsilon_m^f + \varepsilon_m^\theta. \tag{18}$$

2.2. Analysis of OHAM. This approximate analytical method is commonly used for the solution of nonlinear boundary value problem. For justification, consider the following nonlinear boundary value problem.

$$\begin{gathered} E(F(\eta)) + r(\eta) + J(F(\eta)) = 0 \\ C\left(F, \frac{dF}{d\eta}\right) = 0. \end{gathered} \tag{19}$$

In Equation (19), E represents linear operator, J represents the nonlinear operators, $r(\eta)$ represents the known function, $F(\eta)$ represents the indefinite function, and C represents the boundary operative for the defined problem. The deformation equation for OHAM is given below.

$$\begin{gathered} (1-q)\{E(F(\eta, q)) + r(\eta)\} = Z(q)\{E(F(\eta, q)) + r(\eta) + J(F(\eta, q))\} \\ C\left\{F(\eta, q), \frac{dF(\eta, q)}{d\eta}\right\}. \end{gathered} \tag{20}$$

In Equation (20), q represents an implanting parameter, and its range is from 0 to 1, and $Z(q)$ represents a nonzero

Table 6: Comparison for $\theta(\eta)$. And publish work.

η	Numerical	Analytical	Error
1	1	1	0
2	1.21….	1.19….	0.02…
3	1.32….	1.30….	0.02…
4	1.40….	1.35….	0.05…
5	1.54….	1.51….	0.03…
6	1.64….	1.60….	0.04…
7	1.75….	1.70….	0.05…
8	1.50….	1.40….	0.1…
9	1.24….	1.20….	0.04…
10	1.15….	1.10….	0.05…

Table 7: Riahi et al.'s [38] thermophysical properties of silver titanium oxide.

	ρ	k	C_p	β
Silver (Ag)	10.5	429	235	1.89×10^{-5}
Titanium (TiO_2)	4250	8.95	686	0.9×10^{-5}

supplementary function with the $Z(0) = 1$ for $q = 0$ and $q = 1$.

$J_m(F_0(\eta), F_1(\eta) \cdots F_m(\eta))$ are the coefficients of p^m, which are gained by expanding $J(F(\eta, p, D_1 \cdots D_m))$ in the form of power series about the embedding parameter q. Likewise,

$$J(F(\eta, q, D_1 \cdots D_m)) = J\left[F_0(\eta) + \sum_{k\geq} J_k(F_0(\eta), F_1(\eta) \cdots F_k(\eta)) q^k\right]. \tag{27}$$

$J(F(\eta, q, D_1 \cdots D_m))$ is assumed in Equation (26), and the convergence of Equation (26) depends on the auxiliary constant $D_i, i = 1, 2, 3 \cdots$. Equation (27) converges when $q = 1$, and we gain

$$F(\eta, D_1, D_2, \cdots D_m) = F_0(\eta) + \sum_{k\geq 2} F_k(\eta, D_1, D_2 \cdots). \tag{28}$$

We also have $F(\eta, 0) = F_0(\eta)$ and $F(\eta, 1) = F(\eta)$ respectively. Thus, as q increases, from 0 to 1, the solution $F(\eta, q)$ varies from $F_0(\eta)$ to $F(\eta)$.

$$L'(F_0(\eta)) + F(\eta) = 0, \quad B\left(F_0, \frac{dF_0}{d\eta}\right). \tag{21}$$

The power series in q is

$$Z(q) = D_1 q + D_2 q + . \cdots \tag{22}$$

In Equation (22), D_1 and D_2 represent the unknown constant which can be obtained. The required solution is presented as follows:

$$F(\eta, q, D_1 \cdots D_{2m}), \tag{23}$$

$$F(\eta, q, D_1 \cdots D_m) = F_0(\eta) + \sum_{k\geq 1} F_k(\eta, q, D_1 \cdots D_m)\, q^k. \tag{24}$$

Putting Equation (21) in Equation (22) and comparing the coefficients of like power of q primes to the governing equation $F_0(\eta), F_1(\eta)$ up to $F_k(\eta)$,

The m^{th}-order approximation for the problem is

$$E(F_1(\eta)) = D_1 J_0(F_0(\eta)), \quad C\left(F_1, \frac{dF_1}{d\eta}\right) = 0, \tag{25}$$

$$E(F_k(\eta) - F_{k-1}(\eta)) = D_k J_0(F_0(\eta)) + \sum_{i=2}^{k-2} D_i\{E(F_{k-1}(\eta) + J_{k-1}(F_0(\eta), F_1(\eta) \cdots F_{k-1}(\eta)))\} \quad C\left\{F_k, \frac{dF_k}{d\eta}\right\} = 0, k = 1, 2, . \cdots \tag{26}$$

$$F(\eta, D_1, D_2, \cdots D_m) = F_0(\eta) + \sum_{k\geq 1}^{m} F_m(\eta, D_1, D_2 \cdots D_m). \tag{29}$$

The residual error for the problem is

$$R'(\eta, D_1, D_2 \cdots D_m) = E(F(\eta, D_1, D_2 \cdots D_m) + F(\eta) + J(F(\eta, D_1, D_2 \cdots D_m))). \tag{30}$$

$R'(\eta, D_1, D_2 \cdots D_m) = 0$ and $F(\eta, D_1, D_2 \cdots D_m)$ have an exact solution which in overall impossible particularly in nonlinear problems. For $D_i, i = 1, 2, \cdots, m$, we used the

Table 8: Alghamdi et al. [39] show the thermophysical properties.

Properties	Nanofluid	Hybrid nanofluid
Density	$\rho_{hnf} = (1-\phi)\rho_f + \phi\rho_s$	$\rho_{hnf} = \{[(1-\phi_2)(1-\phi_1) + \phi_1 s_1]\} + \phi_2\rho_2$
Heat capacity	$(\rho C_p)_{hnf} = (1-\phi)(\rho C_p)_f + \phi(\rho C_p)_s$	$(\rho C_p)_{hnf}\left[\left\{(1-\phi_2)(1-\phi_1)(\rho C_p)_f\right\} + \phi_1(\rho C_p)_{s_1}\right] + \phi_2\rho(\rho C_p)_{s_2}$
Viscosity	$\mu_{hnf} = \mu_f/(1-\phi)^{2.5}$	$\mu_{hnf} = \mu_f/(1-\phi_1)^{2.5}(1-\phi_2)^{2.5}$
Thermal conductivity	$k_{hnf}/k_{nf} = k_s + (n-1)k_f - (n-1)\phi(k_f - k_s)/k_s + (n-1)k_f + \phi(k_f - k_s)$,	$k_{hnf}/k_{nf} = k_{s_2} + (n-1)k_{bf} - (n-1)\phi_2(k_{bf} - k_{s_2})/k_{s_2} + (n-1)k_{bf} + \phi_2(k_{bf} - k_{s_2})$

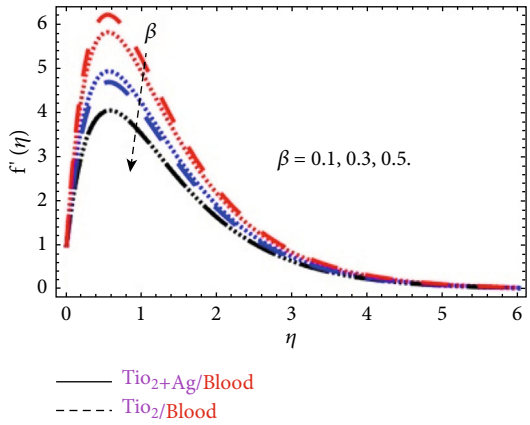

Figure 1: Inspiration of Casson parameter β on velocity profile.

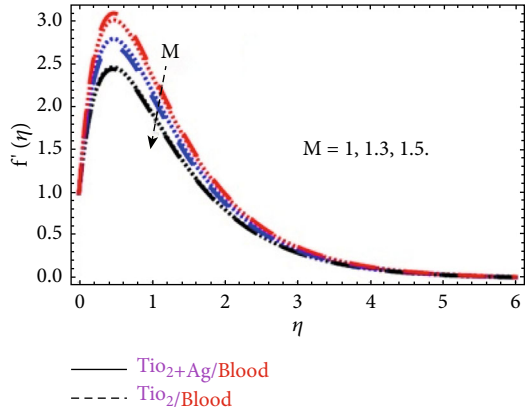

Figure 2: Inspiration of magnetic field parameter M on velocity profile.

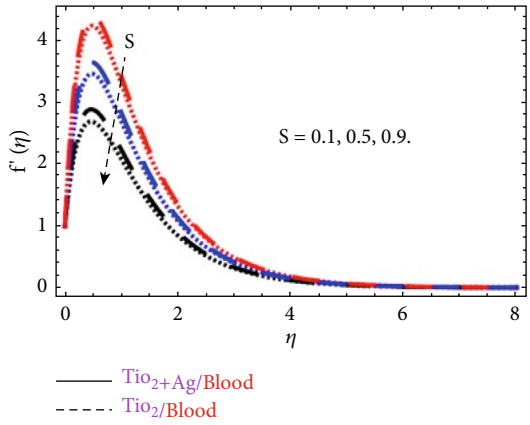

Figure 3: Inspiration of unsteady parameter S on velocity profile.

method of least square.

$$\frac{\partial J}{\partial D_1} = \frac{\partial J}{\partial D_2} \cdots \frac{\partial J}{\partial D_m} = 0, \tag{31}$$

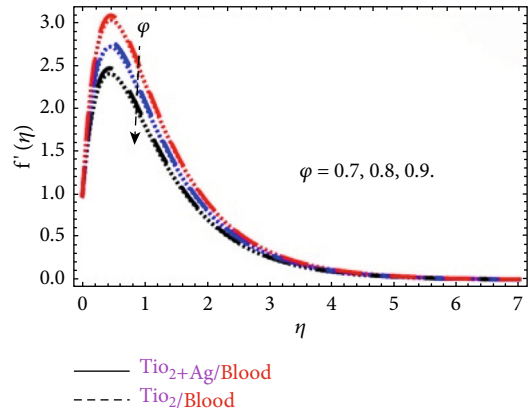

Figure 4: Inspiration of porosity parameter φ on velocity profile.

$$J(D_1, D_2, \cdots D_m) = \int_a^b R'^2(\eta, D_1, D_2 \cdots D_m)d\eta. \tag{32}$$

3. Discussion

In this section, we discuss the effect of different parameters such as β, M, S, φ, Pr, R, G_r, and Ec (Casson parameter, magnetic field parameter, time-dependent parameter, porous medium parameter, Prandtl number, radiation parameter, Grashof number, and Eckert number) on $f'(\eta)$ and $\theta(\eta)$ distribution. The similarity transformation is used to convert the given nonlinear partial differential equation (PDE) to a nonlinear ordinary differential equation (ODE). Two sorts of hybrid nanofluids TiO_2+Ag+blood and TiO_2+-blood are used for the enhancement heat ratio. In the present research paper, TiO_2+blood represents the base fluid and TiO_2+Ag+blood represents hybrid nanofluid. The flow investigation is discussing on a moveable surface along with magnetic field and couple stress along with nonlinear convection. The approximate analytical technique is used to obtain analytical solution of particular problem. The impacts of dissimilar parameter on velocity $f'(\eta)$ and $\theta(\eta)$ are accessible in figures [1–7, 40], the effects on velocity profile are presented in figures [1–4], and the effects of different parameter on temperature profile are presented in figures [5–7, 40]. Tables 1 and 2 represent the impact of different parameters on C_f and Nu for both hybrid nanofluid and base nanofluid. The table shows that C_f (skin friction) coefficient is increasing in both cases for both hybrid nanofluid and base nanofluid. For the increasing values of magnetic field parameter M and Casson parameter β, physically increasing these parameters, viscous force is increasing so as a result, C_f (skin friction) is increasing. Table 2 presents the effect of Ec and R on Nu (Nusselt number) for both hybrid nanofluid and base nanofluid. Nusselt number coefficient is increasing in on both hybrid nanofluid and base nanofluid for growing amount of Ec and R. The convergence of the hybrid nanofluid and base fluid is gained for 25^{th} iteration for both hybrid nanofluid and base nanofluid in Tables 3 and 4. From Tables 3 and 4, we see that growing the iteration decreases the order of residual error and good convergence was achieved. The assessment of the current work and with the

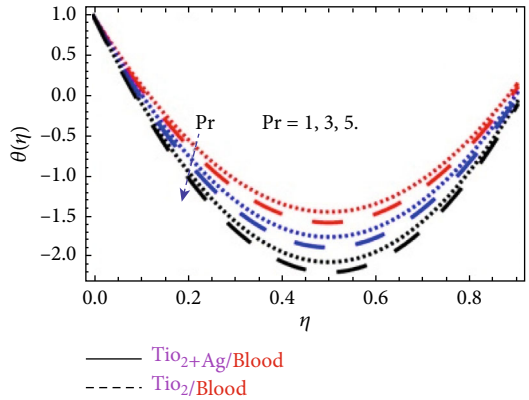

Figure 5: Inspiration of Prandtl number on Pr temperature profile.

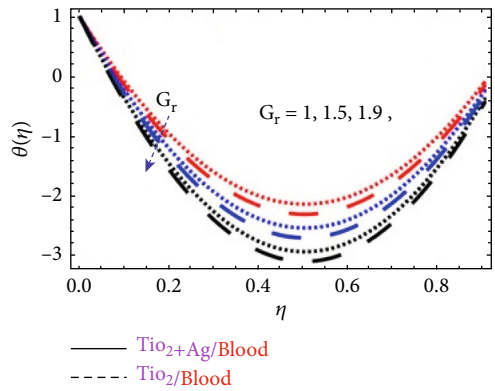

Figure 6: Inspiration of Grashof number G_r on temperature profile.

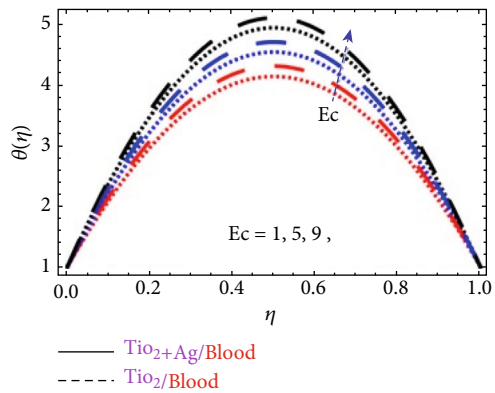

Figure 7: Inspiration of Eckert number Ec on temperature profile.

published research work is obtainable in Tables 5 and 6. Table 7 shows the thermophysical properties of silver titanium oxide. The thermophysical properties of the nanofluid and hybrid nanofluid are presented in Table 8. The variation in Casson parameter β on velocity profile is captured in Figure 1 for both hybrid nanofluid and base nanofluid on $f'(\eta)$, and from Figure 1, we see that $f'(\eta)$ is the declining

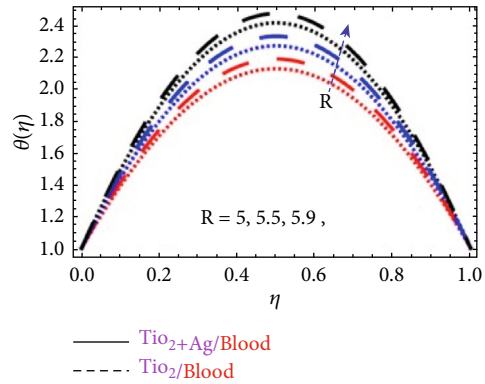

Figure 8: Inspiration of Reedition parameter R on temperature profile.

function of the Casson parameter β. Or there is inverse relation between Casson parameter and $f'(\eta)$ distribution, that is, the growing magnitude of Casson parameter decreases the velocity distribution. This effect is due to construction of resistive forces known as viscous force. The power of this force improves with the increasing power of Casson parameter β which responds the motion of fluid within boundary layer and drops the thickness of boundary layer. The deviation in M (magnetic field parameter) on $f'(\eta)$ profile is captured in Figure 2 for both hybrid nanofluid and base nanofluid on $f'(\eta)$, and from Figure 2, we see that $f'(\eta)$ is the declining function of M. Or there is inverse relation between magnetic field parameter and $f'(\eta)$ distribution, that is, the growing amount of M declarations in $f'(\eta)$ distribution. This effect is due to the production of resistive type force known as Lorentz force. These forces improve with the growing asset of magnetic field parameter M. Due to this, the motion of fluid particles inside boundary layer drops the thickness of boundary layer. The variation in time-dependent parameter S on velocity profile is captured in Figure 3 and for both hybrid nanofluid and base nanofluid, and from Figure 3, we see that velocity is the decreasing function of time-dependent parameter S. The variation in porous medium parameter φ on $f'(\eta)$ profile is captured in Figure 4 for both hybrid nanofluid and base nanofluid on $f'(\eta)$, and from Figure 4, we see that $f'(\eta)$ is the declining function of the porous medium parameter φ or there is inverse relation between porous medium parameter and velocity distribution, that is, the growing magnitude of porous medium parameter decreases the velocity distribution. Such state happens due to the injection and suction of fluid particles. The strength of such force enhances with the rising strength of porous medium parameter φ, which counteracts the motion of fluid within boundary layer and drops the thickness of boundary layer. Figure 5 is schemed for Pr for both hybrid nanofluid and base nanofluid. From Figure 5, we see that $\theta(\eta)$ is the declining function of Pr. We can say that the Prandtl number works as a cooling agent, and this time, the fact is true in the case of hybrid nanofluid other than nanofluids. Figure 6 is schemed for Grashof number G_r for both hybrid nanofluid and base nanofluid. It is noticeable from Figure 6 that the relation between $\theta(\eta)$ and Grashof number G_r is inverse relation,

that is, the large value of Grashof number G_r is declining in temperature distribution as shown in Figure 6. Figure 7 shows the relation between Eckert number Ec and $\theta(\eta)$ is direct relation or $\theta(\eta)$ is the increasing function of Eckert number Ec. Therefore, enhancing the of Eckert number Ec heat is reserved in nanofluid because of the drug or frictional force, and hence, $\theta(\eta)$ enhances. Figure 8 shows the relation between radiation parameter R and temperature profile is direct relation or temperature profile is the increasing function of radiation parameter R Therefore, enhancing the of radiation parameter R heat is reserved in nanofluid because of the drug or frictional force, and hence, $\theta(\eta)$ enhances.

4. Conclusion

This paper investigates approximate analytical study of time-dependent MHD Casson hybrid nanofluid over a stretching sheet along with thermal radiation and on extending surface. Novelty of current research is that the first time-dependent Casson MHD flow of hybrid is addressed for hybrid nanofluid along with variable properties over stretching surface. Transforming nonlinear PDE (partial differential equation) to nonlinear ODE (ordinary differential equation), we used the defined similarity transformation. The governing nonlinear equations are solving with the help of approximate analytical method. The impression of different parameters like couple stress, magnetic field parameter, porous medium parameter, time-dependent parameter, Prandtl number, Grashof number, Eckert number, and radiation parameter is interpreted through graphs for velocity and temperature profile. The key finding of the present research article is as follows:

(1) Growing the value of Casson parameter declarations in velocity

(2) Growing the value of magnetic field parameter declarations in velocity

(3) Growing the value of time-dependent parameter declarations in velocity

(4) Growing the value of porous medium parameter declarations in velocity

(5) Growing the value of Prandtl number declarations in the temperature profile

(6) Growing the value of Grashof number declarations in the temperature profile

(7) Growing the value of Eckert number rise temperature profile

(8) Growing the value of radiation parameter rise temperature profile

Nomenclature

x, y: Cartesian coordinates
u, v: Velocity components
U_w, V_w: Moving surface velocity
S: Unsteady parameter
β: Casson parameter
T: Away from surface temperature
M: Magnetic field parameter
Nu: Local Nusselt number
Pr: Prandtl number
T_w: Sheet temperature
B_0: Continuous magnetic field
T_∞: Ambient temperature
C_f: Skin friction
φ: Porous medium
G_r: Grashof number
R: Radiation parameter
ϕ: Dimensionless concentration
θ: Dimensionless temperature.

Data Availability

The data used to support the findings of this study are available from the corresponding author upon request.

Conflicts of Interest

The authors declare no conflict of interest.

Authors' Contributions

Conceptualization was contributed by A.R and W.K.; methodology was done by A.R., E.B., and W.K; software was contributed by A.R., E.B., and W.K; validation was carried out by A.R., A.A.A.M., and W.K.; formal analysis was performed by A.R. and W.K.; investigation was done by A.R. and W.K.; resources were contributed by A.R.; data corrections were contributed by A.R.; writing—original draft preparation was carried out by A.R.; writing—review and editing was done by A.A.A.M, E.B., and W.K.; visualization was done by A.R., A.A.A.M., and W.K.

Acknowledgments

This Research was supported by the Taif University Researchers Supporting Project Number (TURSP-2020/48), Taif University, Taif, Saudi Arabia.

References

[1] K. S. Mekheimer, "Effect of the induced magnetic field on peristaltic flow of a couple stress fluid," *Physics Letters A*, vol. 372, no. 23, pp. 4271–4278, 2008.

[2] R. Ellahi and A. Riaz, "Analytical solutions for MHD flow in a third-grade fluid with variable viscosity," *Mathematical and Computer Modelling*, vol. 52, no. 9-10, pp. 1783–1793, 2010.

[3] S. Mukhopadhyay and R. S. R. Gorla, "Unsteady MHD boundary layer flow of an upper convected Maxwell fluid past a stretching sheet with first order constructive/ destructive chemical reaction," *Journal of Naval Architecture and Marine Engineering*, vol. 9, no. 2, pp. 123–133, 2012.

[4] S. Nadeem, R. U. I. Haq, N. S. Akbar, and Z. H. Khan, "MHD three-dimensional Casson fluid flow past a porous linearly stretching sheet," *Alexandria Engineering Journal*, vol. 52, no. 4, pp. 577–582, 2013.

[5] A. J. Benazir, R. Sivaraj, and O. D. Makinde, "Unsteady MHD Casson fluid flow over a vertical cone and flat plate with non-uniform heat source/sink," *International Journal of Engineering Research in Africa*, vol. 21, pp. 69–83, 2015.

[6] L. Parmar, S. B. Kulshreshtha, and D. P. Singh, "Effects of stenosis on Casson flow of blood through arteries," *International Journal of Advanced Computer and Mathematical Sciences*, vol. 4, pp. 257–268, 2013.

[7] S. Nadeem, R. U. Haq, and N. S. Akbar, "MHD three-dimensional boundary layer flow of Casson nanofluid past a linearly stretching sheet with convective boundary condition," *IEEE Transactions on Nanotechnology*, vol. 13, no. 1, pp. 109–115, 2014.

[8] I. Ullah, I. Khan, and S. Shafie, "MHD natural convection flow of Casson nanofluid over nonlinearly stretching sheet through porous medium with chemical reaction and thermal radiation," *Nanoscale Research Letters*, vol. 11, no. 1, p. 527, 2016.

[9] A. Kamran, S. Hussain, M. Sagheer, and N. Akmal, "A numerical study of magnetohydrodynamics flow in Casson nanofluid combined with Joule heating and slip boundary conditions," *Results in Physics*, vol. 7, pp. 3037–3048, 2017.

[10] M. Archana, B. J. Gireesha, B. C. Prasannakumara, and R. S. R. Gorla, "Influence of nonlinear thermal radiation on rotating flow of Casson nanofluid," *Nonlinear Engineering*, vol. 7, no. 2, pp. 91–101, 2018.

[11] B. J. Gireesha, M. R. Krishnamurthy, B. C. Prasannakumara, and R. S. R. Gorla, "MHD flow and nonlinear radiative heat transfer of a Casson nanofluid past a nonlinearly stretching sheet in the presence of chemical reaction," *Nanoscience and Technology: An International Journal*, vol. 9, no. 3, pp. 207–229, 2018.

[12] B. Souayeh, M. G. Reddy, P. Sreenivasulu, T. Poornima, M. Rahimi-Gorji, and I. M. Alarifi, "Comparative analysis on non-linear radiative heat transfer on MHD Casson nanofluid past a thin needle," *Journal of Molecular Liquids*, vol. 284, pp. 163–174, 2019.

[13] I. Ullah, K. S. Nisar, S. Shafie, I. Khan, M. Qasim, and A. Khan, "Unsteady free convection flow of casson nanofluid over a nonlinear stretching sheet," *IEEE Access*, vol. 7, pp. 93076–93087, 2019.

[14] M. Abd El-Aziz and A. A. Afify, "Effect of hall current on MHD slip flow of Casson nanofluid over a stretching sheet with zero nanoparticle mass flux," *Thermophysics and Aeromechanics*, vol. 26, no. 3, pp. 429–443, 2019.

[15] S. Suresh, K. P. Venkitaraj, P. Selvakumar, and M. Chandrasekar, "Effect of Al2O3–Cu/water hybrid nanofluid in heat transfer," *Experimental Thermal and Fluid Science*, vol. 38, pp. 54–60, 2012.

[16] S. A. Devi and S. S. U. Devi, "Numerical investigation of hydromagnetic hybrid Cu–Al_2O_3/water nanofluid flow over a permeable stretching sheet with suction," *International Journal of Nonlinear Sciences and Numerical Simulation*, vol. 17, no. 5, pp. 249–257, 2016.

[17] S. P. A. Devi and S. S. U. Devi, "Heat transfer enhancement of Cu–Al_2O_3/water hybrid nanofluid flow over a stretching sheet," *Journal of the Nigerian Mathematical Society*, vol. 36, no. 2, pp. 419–433, 2017.

[18] T. Tayebi and A. J. Chamkha, "Free convection enhancement in an annulus between horizontal confocal elliptical cylinders using hybrid nanofluids," *Numerical Heat Transfer, Part A: Applications*, vol. 70, no. 10, pp. 1141–1156, 2016.

[19] S. S. Ghadikolaei, M. Yassari, H. Sadeghi, K. Hosseinzadeh, and D. D. Ganji, "Investigation on thermophysical properties of Tio2–cCu/H2O hybrid nanofluid transport dependent on shape factor in MHD stagnation point flow," *Powder Technology*, vol. 322, pp. 428–438, 2017.

[20] T. Hayat, S. Nadeem, and A. U. Khan, "Rotating flow of Ag-CuO/H 2 O hybrid nanofluid with radiation and partial slip boundary effects," *The European Physical Journal E*, vol. 41, no. 6, p. 75, 2018.

[21] M. Yousefi, S. Dinarvand, M. E. Yazdi, and I. Pop, "Stagnation-point flow of an aqueous titania-copper hybrid nanofluid toward a wavy cylinder," *International Journal of Numerical Methods for Heat & Fluid Flow*, vol. 28, no. 7, pp. 1716–1735, 2018.

[22] M. Subhani and S. Nadeem, "Numerical analysis of micropolar hybrid nanofluid," *Applied Nanoscience*, vol. 9, no. 4, pp. 447–459, 2019.

[23] D. D. Li, D. F. Keogh, K. Huang et al., "Modeling the response of magnetorheological fluid dampers under seismic conditions," *Applied Sciences*, vol. 9, no. 19, p. 4189, 2019.

[24] L. J. Crane, "Flow past a stretching plate," *Zeitschrift für angewandte Mathematik und Physik ZAMP*, vol. 21, no. 4, pp. 645–647, 1970.

[25] S. Nadeem, R. U. Haq, and C. Lee, "MHD flow of a Casson fluid over an exponentially shrinking sheet," *Scientia Iranica*, vol. 19, no. 6, pp. 1550–1553, 2012.

[26] M. E. Ali and N. Sandeep, "Cattaneo-Christov model for radiative heat transfer of magnetohydrodynamic Casson-ferrofluid: a numerical study," *Results in Physics*, vol. 7, pp. 21–30, 2017.

[27] V. Paresh and R. Ashutosh, "Discussed the dissipative MHD boundarylayer flow in a porous medium over a sheet stretching nonlinearly in the presence of radiation," *Applied Mathematical Sciences*, vol. 4, no. 63, pp. 3133–3142, 2010.

[28] A. J. Chamkha, H. S. Takhar, and V. M. Soundalgekar, "Radiation effects on free convection flow past a semi-infinite vertical plate with mass transfer," *Chemical Engineering Journal*, vol. 84, no. 3, pp. 335–342, 2001.

[29] G. Sandhya, G. Sarojamma, P. V. Satya Narayana, and B. Venkateswarlu, "Buoyancy forces and activation energy on the MHD radiative flow over an exponentially stretching sheet with second-order slip," *Heat Transfer*, vol. 50, no. 1, pp. 784–800, 2021.

[30] L. A. Lund, Z. Omar, I. Khan, D. Baleanu, and K. S. Nisar, "Dual similarity solutions of MHD stagnation point flow of Casson fluid with effect of thermal radiation and viscous dissipation: stability analysis," *Scientific Reports*, vol. 10, no. 1, pp. 1–13, 2020.

[31] W. Ibrahim and T. Anbessa, "Three-dimensional MHD mixed convection flow of Casson nanofluid with hall and ion slip effects," *Mathematical Problems in Engineering*, vol. 2020, Article ID 8656147, 15 pages, 2020.

[32] R. S. Varun Kumar, P. Gunderi Dhananjaya, R. Naveen Kumar, R. J. Punith Gowda, and B. C. Prasannakumara, "Modeling and theoretical investigation on Casson nanofluid flow over a curved stretching surface with the influence of magnetic field and chemical reaction," *International Journal for Computational Methods in Engineering Science and Mechanics*, vol. 23, no. 1, pp. 12–19, 2022.

[33] T. A. Yusuf, F. Mabood, B. C. Prasannakumara, and I. E. Sarris, "Magneto-bioconvection flow of Williamson nanofluid over an inclined plate with gyrotactic microorganisms and entropy generation," *Fluids*, vol. 6, no. 3, p. 109, 2021.

[34] R. N. Kumar, R. P. Gowda, J. K. Madhukesh, B. C. Prasannakumara, and G. K. Ramesh, "Impact of thermophoretic particle deposition on heat and mass transfer across the dynamics of Casson fluid flow over a moving thin needle," *Physica Scripta*, vol. 96, no. 7, article 075210, 2021.

[35] A. Rehman and Z. Salleh, "Influence of Marangoni convection on magnetohydrodynamic viscous dissipation and heat transfer on hybrid nanofluids in a rotating system among two surfaces," *Mathematics*, vol. 9, no. 18, p. 2242, 2021.

[36] A. Rehman and Z. Salleh, "Analytical investigation of magnetic field on unsteady boundary layer stagnation point flow of water-based graphene oxide-water and graphene oxide-ethylene glycol nanofluid over a stretching surface," *Mathematical Problems in Engineering*, vol. 2021, Article ID 8897111, 8 pages, 2021.

[37] S. J. Liao, "An optimal homotopy-analysis approach for strongly nonlinear differential equations," *Communications in Nonlinear Science and Numerical Simulation*, vol. 15, no. 8, pp. 2003–2016, 2010.

[38] A. Riahi, N. Ben–Cheikh, and A. Campo, "Water-based nanofluids for natural convection cooling of a pair of symmetrical heated blocks placed inside a rectangular enclosure of aspect ratio two," *International Journal of Thermal and Environmental Engineering*, vol. 16, no. 1, pp. 1–10, 2018.

[39] W. Alghamdi, T. Gul, M. Nullah et al., "Boundary layer stagnation point flow of the Casson hybrid nanofluid over an unsteady stretching surface," *AIP Advances*, vol. 11, no. 1, article 015016, 2021.

[40] G. T. Thammanna, K. G. Kumar, B. J. Gireesha, G. K. Ramesh, and B. C. Prasannakumara, "Three dimensional MHD flow of couple stress Casson fluid past an unsteady stretching surface with chemical reaction," *Results in Physics*, vol. 7, pp. 4104–4110, 2017.